SUPPLEMENTARY MATERIAL: Interfacial Tension and Surface Pressure of High Density Lipoprotein, Low Density Lipoprotein, and Related Lipid Droplets

O. H. Samuli Ollila[1]
Physical Chemistry,
Lund University, Lund, Sweden
Department of Applied Physics,
Aalto University, Helsinki, Finland

Antti Lamberg
Department of Physics,
Tampere University of Technology, Tampere, Finland

Maria Lehtivaara
Department of Physics,
Tampere University of Technology, Tampere, Finland

Artturi Koivuniemi
Bio- and chemical processes,
VTT, Espoo, Finland

Ilpo Vattulainen
Department of Physics,
Tampere University of Technology, Tampere, Finland
Memphys – Center for Biomembrane Physics, Physics Department,
University of Southern Denmark, Odense, Denmark

[1]Corresponding author.

Simulated systems

For the flat interfaces (Flat1-Flat3), we first constructed a system with the smallest area per molecule, and then systematically increased the simulation box area while keeping the number of molecules in a layer fixed, resulting in systems with different areas per molecule. The smallest box dimensions were 4.4 nm $\times$ 4.4 nm (Flat1, Flat2) and 6.25 nm $\times$ 6.25 nm (Flat3). Each system with a given area per molecule was simulated for 2 μs (Flat1, Flat2) or 24 μs (Flat3). To exclude the role finite size effects we simulated some of the flat systems with three of four times larger box areas which did not essentially effect on the results. Note that the simulation times in this work have been scaled by a factor of 4 to account for the faster effective sampling in MARTINI (34).

As a starting point to construct the systems Droplet1-Droplet5 we used the lipid droplet considered in Ref.(28), which is denoted as LDL-Droplet in Table 1. First, Droplet1 was constructed by removing lipids from LDL-Droplet. The systems Droplet2-Droplet5 with different areas per molecule were then created by removing POPC and LysoPC molecules such that the relative number between POPC and LysoPC lipids remained unchanged. The systems were considered to be equilibrated when there was no reorganization of molecules between core and interface regions, which was monitored by calculating the number of contacts between water and core molecules. For the Droplet1-Droplet3 systems, the number of contacts was essentially unchanged during the entire 3.2 μs simulation, thus this data was used for analysis. For the Droplet4-Droplet5 systems the number of contacts clearly increased during the first 3.2 μs simulation. Thus in these systems we doubled the simulation time to 6.4 μs and used only the last 3.2 μs for analysis.

To study curvature dependence of interfacial tension in interfaces without a surfactant monolayer, we constructed interfaces with different curvature from oil with three different molecular composition: pure TG, HDL-Core, and LDL-Core compositions. First, HDL-Core and LDL-Core systems were constructed by removing free cholesterol, POPC, and lysoPC molecules from HDL-Droplet and LDL-Droplet systems, taken from previous studies (27,28), respectively. Lipids were removed from the LDL-Core system to construct a smaller droplet (LDL-Core-Small) with the same molecular composition. Correspondingly, lipids were added to the HDL-Core system to construct a larger droplet (HDL-Core-Large). Small (TG-Small) and large (TG-Large) droplets consisting of pure TG were made by removing CHES from the HDL-Droplet and LDL-Droplet systems, respectively. The droplets were simulated for roughly 8 μs and equilibrated part of the trajec-

tory (gyration radius and density distributions no longer drifted) was used for analysis (more than 4 μs in each system), except HDL-Core and LDL-Core were simulated for 4 μs and the last 3 μs were used in the analysis. For the flat systems (HDL-Core-Flat, LDL-Core-Flat and TG-Flat) we ran approximately 10 ns equilibration simulation followed by 400 ns production runs.

For the HDL and HDL-Droplet systems the last 4 μs and 2 μs, respectively, of the simulation data taken from previous study (27) was used to calculate the interfacial tensions. Correspondingly, for the LDL and LDL-Droplet systems the last 8 μs and 7.6 μs of the simulation data in Ref. (28) were analyzed, respectively.

Force Fields and Simulation Details

The coarse-grained MARTINI force field (34,35) was used in all simulations. In this semi-quantitative force field, 2-4 heavy atoms are described by a single coarse-grained bead and the interactions between beads are fitted to thermodynamic data. All the details related to the force field can be found from (27,28,33-35).

For the HDL based systems the force field descriptions were directly taken from (27), and for the LDL based systems from (28). For the HDL based systems the pre-release version of MARTINI model was used (27), while for the LDL based systems the final version of MARTINI was employed (28). The models for POPC, lysoPC, and free cholesterol are part of the standard MARTINI force field (34). Coarse-grained models for cholesteryl esters and triglycerides, as well as protein models apoA-I in HDL and apoB-100 in LDL are described in (27) and (28), respectively. The results discussed in this work are essentially the same for the two different LDL models presented in (28), therefore here we discuss the results only for the LDL model labeled as 1 (for details of the LDL models, see discussion in (28)).

All simulations were run with the GROMACS simulation package (36,37). In HDL simulations we used Gromacs 3.3.1, in LDL and LDL-Droplet simulations development version of Gromacs 4.0, and in the rest of the simulations Gromacs 4.0 or a newer version was used. In all simulated models both Lennard-Jones and electrostatic interactions were cut off at 1.2 nm, with shifting from 0.9 nm for Lennard-Jones and from 0 nm for electrostatic interactions. The relative dielectric constant used in simulations was 15. These values are standard MARTINI force field values (34). Time step in all simulations was chosen as 20 fs except for the HDL system where it was 25 fs. In the HDL, HDL-Droplet, LDL, and LDL-Droplet systems

the Nose–Hoover thermostat (38,39) for temperature and the Parrinello–Rahman barostat (40) for pressure were used (compressibility $5\times10^{-5}\text{bar}^{-1}$ and coupling constant 1 ps). In the rest of the systems the Berendsen pressure and temperature coupling schemes (41)were employed (compressibility $5\times10^{-5}\text{bar}^{-1}$ and coupling constant 4 ps). The temperature was set to 310 K in all systems. For spherical systems the pressure was coupled isotropically to 1 bar while in the flat systems the area was kept constant and the pressure in the normal direction was set to 1 bar. Periodic boundary conditions were used in all simulations.

Surface Pressure and Interfacial Tension Calculations for Flat Interfaces

To compare simulated surface pressure-area isotherms to the ones measured by droplet tensiometer experiments, we first calculated γ_0 from a simulation of a pure oil-water interface. Then we simulated a flat monolayer at oil-water interfaces with different values for area per molecule and calculated $\gamma(A)$. The difference then gives $\Pi(A)$ as defined in Eq. 1. The surfactant area per molecule was varied by simulating a system with a fixed number of surfactants but with a varying area in the layer plane.

Interfacial tensions for flat interfaces were calculated by using trilayer simulations (see Fig. 1 A)). In these simulations the simulation box area is kept constant in the layer plane, while the box height is coupled to a pressure of 1 bar. From this setup the interfacial tension can be calculated in a usual manner:

$$\gamma = \frac{L_z}{2}(P_{zz} - \frac{P_{xx} + P_{yy}}{2}), \tag{1}$$

where L_z is the height of the simulation box and $\mathbf{P}$ is the pressure tensor of the whole box (49).

Existence of bulk region inside small droplets

In practice, a clear bulk-like region is found in water outside the droplet (see Fig. 2 A). However, in the core inside the droplet, there are more fluctuations arising from sampling in a spherical geometry as the amount of data is the less the smaller is the radius. These fluctuations would be given a major weight if applied in Eq. 4 due to the r^{-1} term in the denominator. On the other hand, Fig. 2 B shows that the density of the main core lipids (TG, CHES) is roughly constant inside the droplet. Further, an isotropic region inside HDL-like droplets was observed also in a previous work (27), and a

clear bulk region is found inside the larger droplets too, see Fig. 5 B. On these grounds we assume a bulk region to exist also inside small droplets studied in this work.

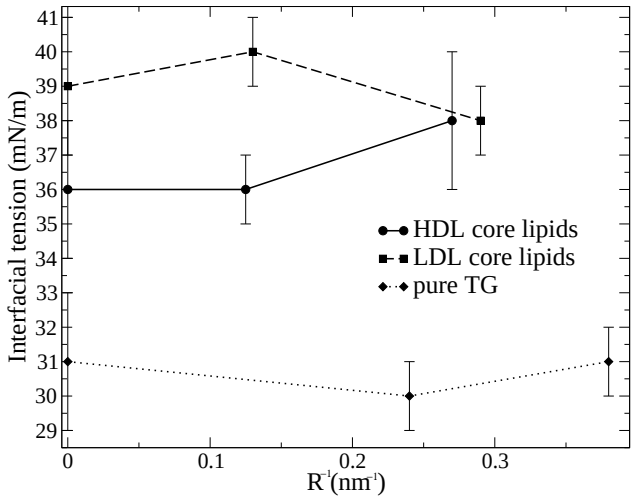

Figure S1: Interfacial tension as a function of curvature for a pure TG (triolein) droplet, and droplets whose compositions match those of HDL and LDL cores.

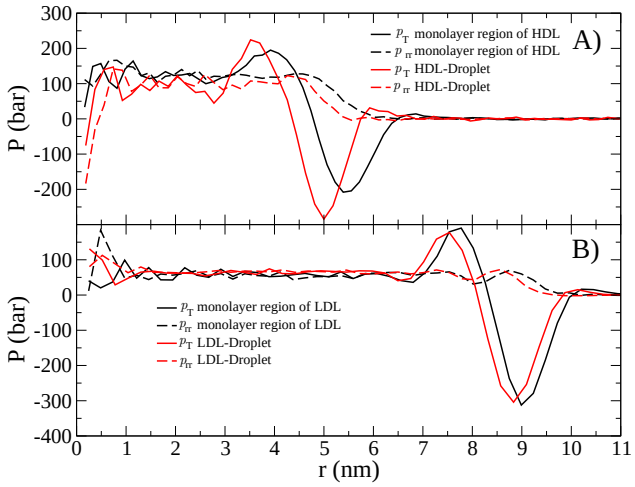

Figure S2: Tangential $p_T(r)$ and radial $p_{rr}(r)$ components of pressure tensor as a function of distance from the center of the particle r, averaged for monolayer regions in A) HDL and B) LDL systems. For comparison the pressure tensor components also for A) HDL-Droplet and B) LDL-Droplet are shown.

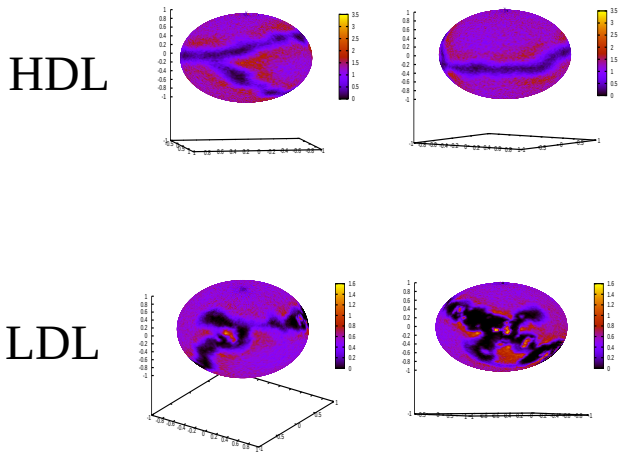

Figure S3: Surface density of PC headgroup beads in spherical coordinates shown from two different angles for HDL and LDL systems. Significantly higher concetrations of headgroups is observed next to the proteins. For surface density calculations the angles in spherical coordinate system are divided into pieces of 1 degree. Then the average number of PC headgroups in each solid angle is calculated and divided by spherical area calculated by using Laplace radius. The usage of Laplace radius is justified since quantitative density values are not important here, only the difference between bulk monolayer and the vicinity of protein.